Modeling Agricultural Load Based on Crop Evapotranspiration and Light Integration for Economic Operation of Greenhouse Power System

Zeming Li, Junyong Liu, *Member, IEEE*, Yue Xiang, *Member, IEEE*, Xin Zhang, *Member, IEEE*, and Yanxin Chai

***Abstract*—The threat of environmental degradation attracts great attention to clean energy production and transportation. However, the limited scope of energy consumption causes large-scale of clean energy sources to be abandoned in Sichuan province. In the meantime, the development of modern greenhouse cultivation has transformed the agriculture industry to have a brand-new type of electrical load in the grid. Consequently, the agricultural load can be used to consume the clean energy while facilitating plant growth. In this paper, an innovative agricultural load model is proposed based on crop evapotranspiration and daily light integration. Furthermore, the proposed agricultural load model is also applied to investigate the electricity consumption of five types of crop planting. The results illustrate that the power consumption is primarily driven by artificial lighting compensation system.**

***Index Terms*—Agriculture load model, Crop evapotranspiration model, Daily light integration model, Power consumption**

I. Introduction

Since the 21st century, the world's science, technology and living standards have continued to develop rapidly, which lead to the significant population growth and urban area expansion. The increased life requirement has brought enormous pressure on the earth's limited resources, including food, water, energy, land and ecosystems [1]. A Food-Water-Energy (FWE) nexus approach has been proposed as a main research topic and global concern in recent years [2].

Moreover, the climate change, the land deforestation desertification, and salinization have caused the instability yields of agricultural production with raising concern on food security [3]. To solve this issue, greenhouse "protected cultivation" can form a relatively stable microclimate that is not affected by external environment, making agricultural production feasible for all seasons without geographical constraints. In addition, the greenhouse's climate control and automation equipment consume electricity at various planting stage with temporal effect. As a result, agricultural production urgently requires sufficient energy supply. Hence, agricultural load has become an important type of load in the power grid.

In recent years, with the development of clean energy generation, the power market in Sichuan has presented a critical situation of oversupply, especially with large-scale redundancy of hydropower. Consequently, a massive amount of water source has been abandoned every year. Hence, under the background of the national power market reform, how to properly consume the surplus hydropower has become the key issue restricting the development of Sichuan power market. Liu et al. [4] intensively analyzed the current problems of the power grid with agricultural load, and the potential of using agricultural load to consume the clean energy. It has been indicated that agricultural load modeling is one of the primary difficulties that drives the success of power and agricultural system integration. In the past, load modeling methods are mainly grouped into two categories: component-based modeling approach and measurement-based modeling approach. Based on component-based approach, an equivalent thermal parameter model of the central air-conditioning system in public buildings considering the thermodynamic characteristics was presented in [5]. Quilumba et al. [6] established a ZIP based household load model considering the utilization of televisions. Considering the time features of load demand, a bottom-up time-variant load model was proposed in [7]. Wang et al. [8] employed wavelet analysis and clustering method to preprocess and classify the load signal, which improved the accuracy of parameter identification of the load modeling. Moreover, a measurement-based composite load model was proposed in [9], while a questionnaire based method was used in [10] for selecting proper load models .

At present, the agricultural load modeling is mainly identified by the measurement-based method, i.e., using the measured data to identify the structure and parameters of the load model. Based on the data measurement, a rural power system load model was proposed by using regression analysis [11]. The agricultural load in Heilongjiang province of China was developed based on neural network with agricultural related power data, which provided a reference for future

This work was supported by the Talents' Training Quality and Teaching Reform Project for 2018-2020 Higher Education in Sichuan Province (JG2018-10) and the New Century Higher Education Teaching Reform Project of Sichuan University under Grant SCU8007

Z. M. Li, J. Y. Liu, Y. Xiang (corresponding author, e-mail: xiang@scu.edu.cn), and Y. X. Chai are with the College of Electrical Engineering, Sichuan University, Chengdu 610065, China.
X. Zhang is with Energy and Power Theme, School of Water, Energy and Environment, Cranfield University, Cranfield MK43 0AL, UK.
DOI: 10.17775/CSEEJPES.2019.00750

agricultural development [12]. However, these load models are based on specific data collection from local system. Therefore, the model only can be applied in specific areas. Besides, the model is data-driven empirical approach which could not deal with microscopic simulation and mechanism analysis of agricultural load characteristics. Furthermore, these models are lack of key factors that fundamentally drive the energy consumption in an agriculture system, which could not provide any contribution to manage and optimize agricultural power load, nor to analyze agricultural load impact on rural distribution network planning. Under this circumstance, based on the crop evapotranspiration and daily light integration modeling, an agricultural load model is established in this paper to optimize and evaluate the electricity consumption and efficiency improvement of five different crops growth in the solar greenhouse.

II. Modeling of Crop Growth with Environmental Factors

The solar greenhouse constructs a suitable environment for crop growth with required soil, water, and climate resources to increase plant productivity and quality, with opportunities to enhance market supply for all seasons. In the greenhouse environment, there are many coupled environmental factors that influences the crop growth, mainly including soil moisture, illumination, temperature, carbon dioxide concentration, and humidity, which make the greenhouse as a complex system. In this paper, illumination and soil moisture, which are correlated to the electricity supply, are analyzed and discussed.

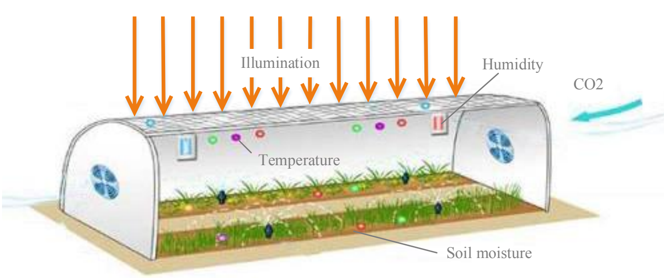

Fig.1. Environmental factors to impact plant growth in the greenhouse.

A. Illumination

As the major energy source of greenhouse ecosystem, sunlight is the vital nature source for the photosynthesis process of plants. The crop uses the photosynthetic pigments in the body to capture the energy from the sunlight to meet the energy requirements of various life activities. Sufficient sunlight is in favor of organic matter accumulation in the crop itself, promoting crop growth and increasing dry weight of crops. Furthermore, lighting also effectively controls the various life activities in plants, such as the photoperiod of plants can induce crop flowering, dormancy and vegetative growth [13-14]. Moreover, the illumination quality of the light source can promote compound various pigments in the body of crop, improve the quality of crops, and increase the market competitiveness and value of crops [15].

In order to evaluate the quantity of power required in the illumination system, it is necessary to know the light required for crop growth. There are many ways to measure the light intensity of various light sources, such as footcandles, lux, lumens, etc. However, none of these methods are commonly accepted in the field of agriculture. At present, the daily light integral (DLI) recommended by the American Horticultural Society is commonly used to describe photosynthetically active radiation (PAR) associating with photosynthesis process of plant growth, measured by mol/ ($m^2 \cdot d$) [16]. The mathematical representation is shown as follow [17]:

$$DLI = L_{\text{intensity}} \cdot Light_{\text{cycle}} \cdot 3600/10^6 \quad [mol \cdot m^{-2} \cdot d^{-1}] \tag{1}$$

where $L_{\text{intensity}}$ is the light intensity. $Light_{\text{cycle}}$ is the time period.

The plants can be typically categorized into five types, which are very low light (less than 5 mol/m^2/d), low light (5–10 mol/m^2/d), moderate light (10–20 mol/m^2/d), high light (20–30 mol/m^2/d), and very high light (30–60 mol/m^2/d). According to the required DLI for each type of plant which is appropriate to its growth [18], a DLI between 4 to 12 mol/m^2/d is the typical range for plant growth and development [19]. However, due to the variation in latitude, cloud cover and haze density, the direct sunlight has reduced effect on plant growth. Consequently, it is often unable to achieve the optimal lighting environment for plant growth in nature environment. Therefore, artificial lighting compensation has become an effective solution to improve the plant illumination environment, and reduce the crop growth cycle [20].

At the meantime, the light absorption ability of plants is limited. When the light is too strong, the large amount of solar energy accumulated on the leaves will cause the plant surface temperature to raise at a high level and burn the leaves. This would reduce the photosynthetic rate of the plants and adversely affect their growth which is called as light saturation phenomenon. Therefore, the plant light saturation point can be used as the most suitable light intensity, and become the target DLI to maximize daily plant growth with no energy waste. Due to climate and environmental factors, when natural light cannot meet the amount of light required for plant growth, the artificial light compensates the light shortage, which is represented in equation (2).

$$DLI_{\text{compensation}} = DLI_{\text{target}} - DLI_{\text{sunlight}} \tag{2}$$

where DLI_{sunlight} is the amount of natural sunlight, which can be derived by professional equipment. $DLI_{\text{compensation}}$ is the light compensation from artificial source, and DLI_{target} is the target light that can be calculated by equation (3), with the LSP (light saturation point) indicating the point of light saturation [18].

$$DLI_{target} = \text{mean } LSP \text{ at } 70\% \text{ max photosynthesis} \times 0.0432 \tag{3}$$

Currently, the LED light is widely used in greenhouse artificial lighting compensation system [21]. The electricity consumption of artificial lighting system can be described as a function of the required compensation light amount, the power output of LED and the light illumination per unit power, as shown in the following equation:

$$P_{\text{light}} = \iint \frac{DLI(x,y)}{DLI_{\text{light}}} \cdot P_{\text{LED}}(x,y)\,dxdy \tag{4}$$

where $DLI(x, y)$ represents the distribution of DLI required for crop growth within the greenhouse, which is equal to $DLI_{compensation}$ in each time period; DLI_{light} is the amount of DLI emitted by the unit power of the LED, and $P_{LED}(x, y)$ illustrates that the distribution of LED load in the greenhouse.

B. Soil Moisture

Freshwater is an important component containing in the plant body, which plays an important role in the various life activities of plant. Irrigation system is commonly used in greenhouse to supply water and maintain soil moisture for the plants. To establish the load model of irrigation system, the crop daily water requirement for growth is measured.

The plant water requirement mainly consists of transpiration (T), evaporation (E) and the water that constitutes the plant body. Since the water retained in the plant is only a small proportion comparing with the water lost through evaporation, the water in plant will be ignored when estimating the water requirement. The combination of two separate processes whereby water is lost on the one hand from the soil surface by evaporation and on the other hand from the crop by transpiration is referred to as evapotranspiration (ET) [22].

The evapotranspiration of crops can be directly derived by using instrument measurement or experience formulas. However, such expensive measurement or empirical formulas are not satisfied for the theoretical analysis. So, Penman-Monteith model [23] is utilized to precisely calculate evapotranspiration, which is based on the energy balance theory and turbulent diffusion theory (the energy flow in farmland is shown as Fig.2).

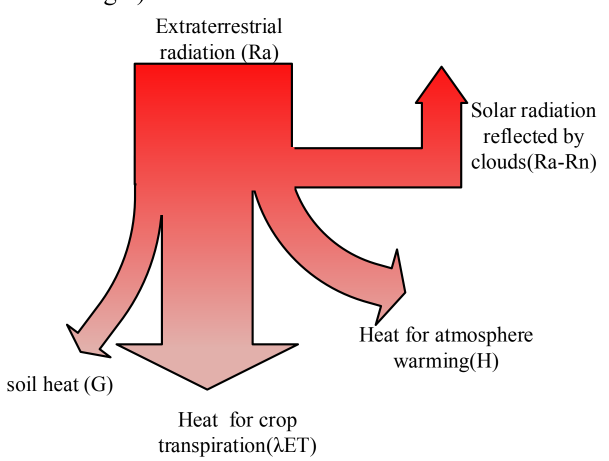

Fig.2. Solar radiation energy transfer map in farmland, whereby the energy balance is described as: $R_n = \lambda ET + H + G$.

However, the parameters of surface resistance and aerodynamic resistance are too complicated to calculate in the model [24], which makes the impractical application of the model. Therefore, this paper adopts the widely applied dual crop coefficient model [25]-[29] which is modified from the Penman-Monteith model by Food and Agriculture Organization of the United Nations (FAO) to calculate the crop evapotranspiration as shown in equation (5), and the parameters in this model are discussed below.

$$\begin{aligned} ET_0 &= ET_{rad} + ET_{aero} \\ &= \frac{0.408\Delta(R_n - G)}{\Delta + \gamma(1+0.34U_2)} + \frac{\gamma \cdot 900 \cdot U_2(e_s - e_a)}{(\Delta + \gamma(1+0.34U_2)) \cdot (T+273)} \\ ET_c &= K_c \times ET_0 = (K_s K_{cb} + K_e) ET_0 \end{aligned} \tag{5}$$

Where ET_{aero} and ET_{rad} represent radiation term of crop evapotranspiration and aerodynamic term of crop evapotranspiration respectively. R_n represents solar radiation. G represents the soil heat flux. e_s and e_a represent saturated vapour pressure and ambient vapour pressure respectively. γ represents psychrometric constant. Δ, U_2 represent the slope of the saturated vapor pressure curve and the wind speed at 2 m above the ground surface, respectively. T represents average air temperature. ET_c, defined as the crop evapotranspiration under standard conditions, is the evapotranspiration from disease-free, well-fertilized crops, grown in large fields, under optimum soil water conditions, and achieving full production under the given climatic conditions. ET_0 is called reference crop evapotranspiration. K_c represents crop coefficient, which scales the reference evapotranspiration to explain specific effects of crops on evapotranspiration and variation in different crop growing season. K_{cb} is the basal crop transpiration coefficient, K_s is the water stress coefficient (0-1) that shows the plant water status, and K_e is the evaporation coefficient. The value of K_{cb} under standard climatic conditions (daily minimum relative humidity RH_{min} =45% and wind speed at 2m U_2 =2 m/s) is available through the basic crop coefficient table provided by FAO, and can be corrected using the equation (6) for non-standard climatic conditions.

$$\begin{aligned} K_{cb} = K_{cb} + [0.04(U_2 - 2) - 0.004(RH_{min} \\ - 45)](\frac{h}{3})^{0.3} \end{aligned} \tag{6}$$

The solar radiation R_n in equation (5) is corresponding to the difference between the incoming short-wave radiation R_{ns} and the outgoing long-wave radiation R_{nl}, derived by the equation (7).

$$\begin{aligned} R_n &= R_{ns} - R_{nl} \\ &= 28.952 \cdot d_r \cdot (0.25 + 0.5n/N)(W_s \cdot \sin(\varphi) \cdot \sin(\delta) \\ &\quad + \sin(W_s) \cdot \cos(\varphi) \cdot \cos(\delta)) - 2.45 \times 10^{-9} \cdot (0.9n/N \\ &\quad + 0.1) \cdot (0.34 - 0.14\sqrt{e_a}) \cdot (T_{kx}{}^4 + T_{kn}{}^4) \end{aligned} \tag{7}$$

where d_r and δ are the inverse relative distance Earth-Sun and the solar declination respectively. Those are functions of the Julian day number J, given as the formula (8) and (9), and W_s represents the sunset hour angle, which is obtained by the equation (10). T_{kx} is maximum absolute temperature and T_{kn} is minimum absolute temperature. e_a is the ambient vapour pressure. n represents the actual duration of sunshine. N represents the maximum possible duration of sunshine or daylight hours, and φ is latitude.

$$\delta = 0.409 \cdot \sin(0.0172J - 1.39) \tag{8}$$

$$d_r = 1 + 0.033\cos(0.0172J) \tag{9}$$

$$W_s = \arccos(-\tan\varphi \cdot \tan\delta) \tag{10}$$

Saturated vapour pressure e_s and ambient vapour pressure e_a in equation (5), are calculated by equation (11). In particularly, when the relative saturation humidity RH=100, the ambient vapor pressure becomes e_s.

$$e_a = 0.611\exp(\frac{17.27T}{T+237.3})\cdot\frac{RH}{100} \quad (11)$$

Soil heat flux G in equation (5), can be simplified by the temperature difference shown as equation (12), where T_d and $T_{d\text{-}1}$ are the temperature of intra-day d and previous day d-1, respectively.

$$G = 0.38(T_d - T_{d-1}) \quad (12)$$

The psychrometric constant γ in equation (5), can be derived by equation (13).

$$\gamma = \frac{C_p P}{\varepsilon\lambda}\times 10^{-6} \quad (13)$$

where C_p is the specific heat of the humid atmosphere, taking 1.013KJkg^{-1}℃$^{-1}$, ε represents the ratio molecular weight of water vapour/dry air, taking 0.622 [30]. The atmospheric pressure P is a function of altitude, and λ represents the latent heat of vaporization, which is a function of temperature.

The slope of the saturated vapor pressure curve Δ in equation (5) can be obtained from the formula (14).

$$\Delta = \frac{4098\cdot e_a}{(T+237.3)^2} \quad (14)$$

Once the daily water demand of the plant is modelled, it is necessary to link between water demand and power demand, which is given in [31]. This equation models the electric load of the irrigation system:

$$P_{irrigation} = E_h \times (\frac{100}{\eta}) = V \times H \times (\frac{\rho \times g}{3600}) \times (\frac{100}{\eta}) \quad (15)$$

where:

$P_{\text{irrigation}}$=the power of the drip irrigation system[W].

E_h = hydraulic energy[kWh].

V= the volume of water, is the amount of water required for irrigation by drip irrigation system in each hour (ET_c) [m^3/h].

H= the pumping head of water [m].

g= standard gravity [9.8 ms^{-2}].

η= motor-pump efficiency [%].

ρ=density of water [1000kgm^{-3}].

III. Simulation of Agricultural Load Model in Greenhouse System

A power system is designed to simulate agricultural load of greenhouse with energy storage and renewable power generation. The greenhouse's power is supplied by the grid and a photovoltaic (PV) power generation system. An energy storage system is applied to absorb excessive PV generation, and provide additional power to the greenhouse. For agricultural load modeling, the irrigation system and artificial lighting compensation system are mainly made into consideration on the load side of the greenhouse. In order to simplify the complexity of the system, the temperature and humidity control with ventilation and cooling load modeling are not considered.

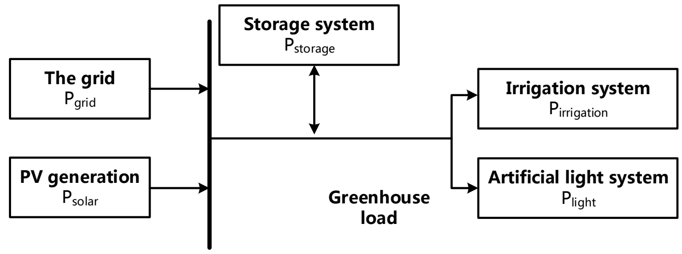

Fig.3. Power system simulation with greenhouse load, PV generation and energy storage system.

The grid is assumed to be an infinite bus power system that constantly maintain the power balance to meet demand. Three locations (Chengdu, Jinan, and Haikou) with five common crops (i.e., lettuce, cabbage, sweet pepper, cucumber, and tomato) are selected as agricultural samples for simulation. The geographical, climate and crop parameters involved in the simulation are shown in Table Ⅰ and Ⅱ.

TABLE Ⅰ
THE GEOGRAPHICAL INFORMATION OF THREE CITIES

Location	Latitude(°)	Altitude(m)	Actual duration of sunshine(h)
Chengdu	30.67	600	2.87
Haikou	20.03	14.1	3.75
Jinan	36.68	51.6	4.44

TABLE Ⅱ
THE CROP PARAMETERS OF FIVE CROPS

Crop	K_{cb}	Target DLI
Lettuce	0.95	14.51
Cabbage	0.9	17.35
Tomato	1.1	28
Sweet pepper	1	15
Cucumber	0.95	17.5

To model the hourly agricultural load, the total daily amount of light compensation and water consumption are required to be satisfied, as shown in equation (16). Meanwhile, it is assumed that the irrigation and light compensation load can be timely adjusted in a day in accordance with the actual crop growth mechanism.

$$\sum_i^n ET_i = ET_c\ ,\ \sum_i^n DLI_i = DLI_{\text{compensation}} \quad (16)$$

ET_i, DLI_i represent the amount of irrigation and light compensation for the period i. The water amount in each irrigation period needs to meet the constraints of irrigation regulation, which guarantees that the soil moisture is maintained in a range between soil water holding capacity (field capacity) and wilting point. The maximum light compensation at each time period is limited by the full power output of LED, as shown in equation (17).

$$ET_i \in (D_{emin}, D_{emax}),\ DLI_i \in (0, DLI_{imax}) \quad (17)$$

where $D_{e\min}$ and $D_{e\max}$ represent the minimum and maximum evaporation depth under the irrigation regulation. $DLI_{i\max}$ is the maximum DLI output.

In the design of artificial light compensation system, excessive light energy would not be absorbed by plants, and

This article has been accepted for publication in a future issue of this journal, but has not been fully edited. Content may change prior to final publication.

further illumination would also have risks to burn the leaves. Thus, the light compensation system would be switched off during the daytime when the nature sunlight is sufficient to save energy. To follow the actual crop growth law, the control logic for light compensation system considering the photoperiod is shown as follows,

$$\begin{cases} XL_i = 0 & (i \in C \cup U) \\ XL_i = 1 & (i \in \overline{C} \cap \overline{U}) \end{cases} \tag{18}$$

where XL_i is a binary variable (0 or 1) indicating whether the light compensation system can be used in hour i over the whole day period. C represents the cycle of dark period still required for the necessary crop life activities, and U represents the time when the sunlight is sufficient.

The battery energy storage system (BESS) is set to store redundant PV generation, and discharge when the system generates insufficient power. Model (19) describes charging and discharging characteristics of the BESS:

$$\begin{aligned} & E_{\mathrm{B}}(t) = E_{\mathrm{B}}(t-1) + P_{\mathrm{BC}}(t)\cdot \eta_c \cdot \Delta t - P_{\mathrm{Bd}}(t)/\eta_d \cdot \Delta t \\ & E_{\mathrm{Bmin}} < E_{\mathrm{B}}(t) \le E_{\mathrm{B}} \end{aligned} \tag{19}$$

where $E_{\mathrm{B}}(t)$ is the energy stored by the battery; η_c and η_d are the charging and discharging efficiency of the battery respectively; $E_{B\mathrm{min}}$ is the minimum of the battery storage capacity; E_{B} is the rated energy storage capacity; P_{BC}, P_{Bd} is the charge and discharge power.

The power balance equation of the whole system during the operation of greenhouse is as following:

$$P_{solar} + P_{\mathrm{grid}} = P_{\mathrm{storage}} + P_{\mathrm{light}} + P_{\mathrm{irrigation}} \tag{20}$$

where P_{solar}, P_{grid}, P_{storage}, P_{light}, $P_{\mathrm{irrigation}}$ are the power of the photovoltaic system, the purchased power of the external power grid, the charge-discharge power of storage system, the load of artificial lighting compensation system, and the load of the irrigation system, respectively. Due to the fluctuation of the supply and demand in the grid, the electricity price is not constant within a day, which has a peak-to-valley price difference. Considering the economic operation of the green house with agricultural load, the optimization objective is to minimize the total cost of power purchase from external grid when operates the day-ahead optimization design, which is shown in (21), with $C(t)$ represents time-of-use electricity price during the period t.

$$minF = \sum P_{\mathrm{grid}} \cdot \Delta t \cdot C(t) \tag{21}$$

TABLE III
THE IRRIGATION WATER DEMAND

Crop	Water demand (mm)		
	Chengdu	Haikou	Jinan
Lettuce	3.06806	3.83155	3.00727
Cabbage	2.95445	3.68964	2.89589
Tomato	3.40898	4.25727	3.34142
Sweet pepper	3.18172	3.97346	3.11866
Cucumber	3.06809	3.83155	3.00727

The daily water demand of five crops at three locations are calculated for a 1000 m^2 greenhouse system by the crop evapotranspiration model proposed above, and the results are shown in Table III. The results indicate that evapotranspiration of crops in different places varies with geographical conditions. Haikou requires the largest water demand because of strong sunshine, low latitude and high average annual temperature, which accelerates the evapotranspiration of crops, followed by Chengdu. Owing to the high latitude and low altitude, crops in Jinan requires the least water for irrigation. The amount of water required for irrigation is expressed in millimeters. If the density of the water is 1000 kg/m^3, for example, around 3.068, 3.832, 3.007 tons of water is needed for lettuce irrigation in a 1000 m^2 (1.5 mu) greenhouse.

Based on (1), the daily lighting compensation of the five crops at different locations is shown in Table IV measured by hours. When estimating the amount of light compensation of tomato planting, it was found that the LED with 20W could not provide sufficient light compensation to satisfy the photoperiod demand of the plant, so the power of the LED lamp was doubled, thus the load was doubled.

TABLE IV
THE LIGHT REQUIRED TO BE COMPENSATED

Crop	Lighting compensation (hour)		
	Chengdu	Haikou	Jinan
Lettuce	4.1759	2.263	0.963
Cabbage	6.806	4.893	3.593
Tomato	8.3333	7.377	6.727
Sweet pepper	4.6296	2.717	1.417
Cucumber	6.9444	5.031	3.732

According to the calculated daily water demand and light compensation hours of crops, the cost-effectively daily distribution of the irrigation water and lighting compensation for five plants in Chengdu is shown in Fig.4. These results are calculated by implementing the proposed optimization methods of the irrigation and light compensation systems.

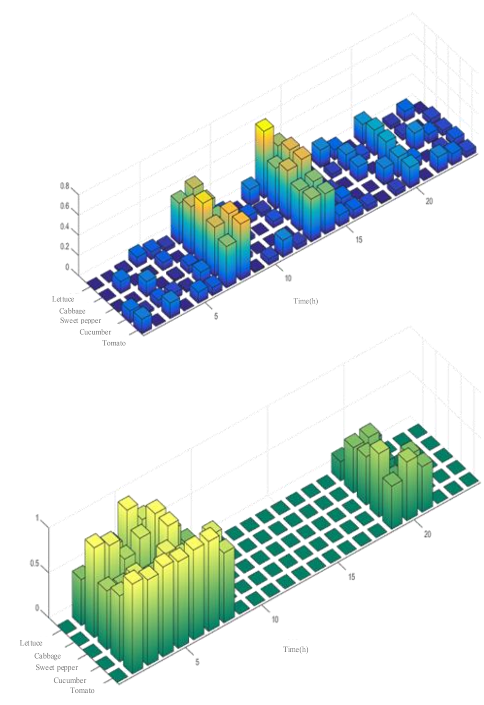

Fig.4. The daily distribution of the required irrigation water and lighting compensation for five plants in Chengdu

This article has been accepted for publication in a future issue of this journal, but has not been fully edited. Content may change prior to final publication.

The results illustrate that the irrigation system is mainly restricted by the irrigation regulation required by crop growth. The irrigation water is mainly concentrated at noon and morning to avoid crop water shortage caused by excessive evaporation. Irrigation is less required at night to reduce the potential waste of water. However, the irrigation system is less responsive to the electricity price as the main purpose of irrigation is to maintain the crop growth. In contrast, the behavior of lighting compensation system will be changed due to the fluctuations of electricity price to save the electricity purchase cost from grid, while still satisfying the essential constraints. As a result, the light system is mainly performed at midnight when electricity price is low and the nature sunshine is unavailable. However, there is also plenty of available lighting compensation achieved by the solar energy stored in the battery during the high price period of the evening.

Fig.5 shows that the load dispatch of both irrigation and light systems are responsive to the electricity price. In addition, the electricity consumption curve of the greenhouse is in accordance with the light compensation system load curve, indicating that the electricity consumption of the irrigation system is much less than that of the light compensation system. The light compensation system average power is 5671.7W, while irrigation system average power is only 126W. Therefore, electricity consumption characteristics of the greenhouse are primarily determined by the light compensation system.

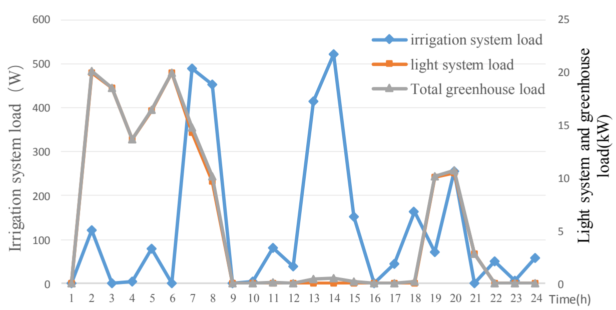

Fig.5. The optimal greenhouse load curves in response to electricity price

The numerical data above describes the circumstance that crops is in the midseason of growth period. When the crop is in different growth period, the parameters are various in the model. In model (5), according to the definition of crop coefficient, the parameter K_c can effectively reflect the difference in water demand of different plants in different growth cycles or different plants. In model (2), DLI_{target}, which represents the target light, will vary with crop type and growth period. Therefore, these two critical parameters of our agricultural load can be used to represent different growth stages and crop type. And the results are shown in Table Ⅴ. The data indicates that in midseason stage the more water and irrigation load needed than in the initial stage or end season stage, because of the largest crop coefficient in the midseason. And also, the midseason growth stage of all crop requires the most illumination, so the light compensation load is highest compared with the other stages. From the results, we can know that tomato is the most energy-intensive crop among these five crops, owing to the most irrigation and light compensation requirements. Particularly, due to lettuce in end season requires less light, so it don't need light compensation. In order to further compare the advantages for the optimal operation of agricultural load in a greenhouse system, a traditional power usage behavior is designed according to the traditional agricultural planting experience. The amount of irrigation water is shown in Table Ⅵ, while the lighting system continuously compensates illumination from 18 o'clock until the time of daily growth sunlight of the crop is satisfied.

TABLE Ⅵ
THE IRRIGATION WATER IN TRADITIONAL PLANTING MODE

City	Crop	Irrigation water volume(mm)		
		8:00am	12:00am	20:00pm
Chengdu	Lettuce	0.7	1.8	0.6
	Cabbage	0.6	1.8	0.6
	Sweet pepper	0.7	1.9	0.6
	Cucumber	0.8	1.6	0.6
	Tomato	1	1.8	0.6
Haikou	Lettuce	1.3	2	0.5
	Cabbage	1.2	1.9	0.6
	Sweet pepper	1.3	2	0.6
	Cucumber	1.3	1.9	0.7
	Tomato	1.4	2.1	0.7
Jinan	Lettuce	1	1.5	0.5
	Cabbage	0.9	1.4	0.6
	Sweet pepper	1	1.6	0.6
	Cucumber	1	1.5	0.5
	Tomato	1.1	1.7	0.6

TABLE Ⅴ
AGRICULTURAL LOAD IN DIFFERENT GROWTH PERIOD

	Initial		Midseason		End season	
	Irrigation(W)/ K_c	Light compensation(kW)/ Target DLI	Irrigation(W)/ K_c	Light compensation(kW)/ Target DLI	Irrigation(W)/ K_c	Light compensation(kW)/ Target DLI
Lettuce	1308.64/0.15	—/10.35	3132.00/0.95	83.52/14.51	2900.00/0.85	—/10.35
Cabbage	1308.64/0.15	88.52/14.78	3016.00/0.9	13.61/17.35	3016.00/0.9	88.52/14.78
Tomato	1308.64/0.15	25.93/24	3480.01/1.1	33.33/28	2668.00/0.75	25.93/24
Sweet pepper	1308.64/0.15	37.04/12	3248.00/1.0	92.59/15	2784.00/0.8	37.04/12
Cucumber	1308.64/0.15	37.04/12	3132.00/0.95	13.89/17.5	2552.00/0.7	37.04/12

The cost comparison between the optimal operation mode and the traditional planting mode is shown in Table Ⅶ. According to five different types of crops at three different planting locations, the daily electricity cost savings is achieved in the range of 4.2-28.5 yuan per day, with the savings of electricity proportion from 75.93% (the lettuce cultivation in Jinan) to 12.57% (the tomato planting in Chengdu). From the numerical data, tomato planting is high-cost in all locations, costing 143, 119, 108 yuan per day in optimal operation mode. The reason for that is because tomato growth requires more light compensation than other crops, showing in Table Ⅳ. That means tomato planting needs more power to satisfy its growth, which is not suitable for the power shortage area. On the contrary, lettuce is a low-cost type of crops, especially in high latitude area. Compared with lettuce cultivation, tomato cultivation has a significant improvement in the cost of electricity, but its saving ratio is low, which is mainly caused by the wide variety of biomass demand of the crop itself. The results could provide a reference for suitable crop type selection at different cities for the economic operation of greenhouse system considering the agricultural load modeling.

TABLE Ⅶ
ELECTRICITY COST COMPARISON

City	Crop	Cost in optimal mode (yuan / day)	Cost in traditional mode (yuan / day)
Chengdu	Lettuce	26.818	40.984
	Cabbage	52.055	64.357
	Sweet pepper	32.101	45.182
	Cucumber	55.394	65.727
	Tomato	143.100	163.677
Haikou	Lettuce	12.575	19.399
	Cabbage	35.766	48.009
	Sweet pepper	16.629	25.115
	Cucumber	35.851	49.436
	Tomato	119.399	147.953
Jinan	Lettuce	1.328	5.519
	Cabbage	23.023	34.999
	Sweet pepper	5.101	8.707
	Cucumber	24.868	36.603
	Tomato	108.757	136.378

The purchased electricity from the grid is divided to three categories: plain electricity, peak electricity and valley electricity. The ratio of daily purchased power consumed by different crops at the greenhouse in either optimal operation mode or traditional operation mode are illustrated in Fig.6, while Fig.6(a) illustrates that in Chengdu, Fig.6(b) and Fig.6(c) indicate Jinan and Haikou respectively. The results show that crop planting uses more than 60% off-valley power in traditional customs. But after optimization, the working time of the artificial light shifts from peak periods to valley periods, which improves the power usage structure. Particularly, in Chengdu, there is a distinct change of electricity consumption structure of lettuce planting, which is 15.8% plain electricity and 84.2% peak electricity to 99.99% valley electricity and trace of plain electricity and peak electricity, as seen in Fig.6(a). Wherever the crop plants in, the electricity used in the growth process includes over 75% valley electricity after optimization. What is important is this electricity consumption structure is more amicable to the grid. Compared with the traditional operation mode, the optimal one could consume more power in valley periods and less power in peak periods, which is beneficial to absorb abandoned hydropower in the valley and reduce the peak and valley difference for smoothing power system operation.

Fig.6. The ratio of daily purchased power consumed by different crops at the greenhouse, (a) in Chengdu, (b) in Jinan and (c) in Haikou

Further research announced by Li et al. indicated that the yield and market price of crops had a significant impact on the return of investment in greenhouses, based on the analysis of five PV greenhouses with Annual Return on Investment (AROI) method [32]. In order to provide a more comprehensive reference for economic benefit of optimal greenhouse operation located in different cities. Factors including crop yield, growth cycle and wholesale market price have been taken into consideration. The information of yield, growth cycle and market price of each crop was collected from the China Agricultural Information Network [33], shown in the Table Ⅷ.

TABLE Ⅷ

THE AGRICULTURAL INFORMATION OF CROPS

Crop	Yield(kg/m2)	Life cycle(d)	Location	Market price(yuan/kg)
Lettuce	5.25	60	Chengdu	4.4
			Jinan	3.5
			Haikou	4
Cabbage	6.75	55	Chengdu	1.3
			Jinan	1.6
			Haikou	2.4
Sweet pepper	7.5	210	Chengdu	8.4
			Jinan	10.88
			Haikou	7.8
Cucumber	9	90	Chengdu	3.4
			Jinan	2.6
			Haikou	3.6
Tomato	30	150	Chengdu	5.6
			Jinan	7
			Haikou	5.2

The cultivation daily earnings in optimal greenhouse operation is shown in Fig.7 and the economic improvement of crop planting in Chengdu, Jinan, and Haikou is shown in Fig.8. As it can be seen from Fig.7, the tomato cultivation final earnings are greater than the other four crops because of its high yield and market price, although it has a highest daily electricity cost. Compared with the electricity cost shown in Table Ⅵ, after the optimization, the influence of electricity cost of lettuce planting is the most positive, reducing by 75.93% in Jinan, while the improvement of planting income is not obvious as expected, increasing by 4.12% in Chengdu, 1.39% in Jinan, and 2.06% in Haikou. The results indicate that for same planting location, the planting economic improvement is affected by the crop types. In Chengdu area the most appreciable improvement is sweet pepper planting at 5.13%, while in Jinan and Haikou area is cabbage planting at 7.42% and 4.97% respectively. Because tomato is a high yield kind of crop, the highest-earning will be taken from tomato planting among these three areas.

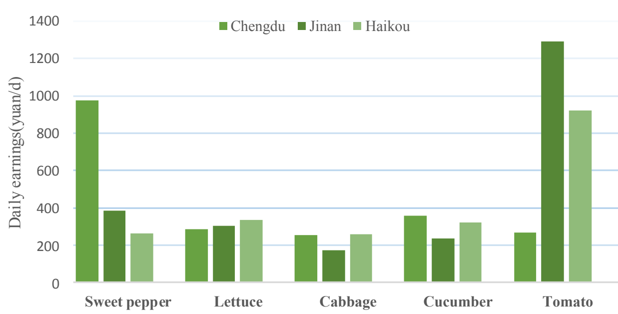

Fig.7. The crop planting daily earnings in optimal operation

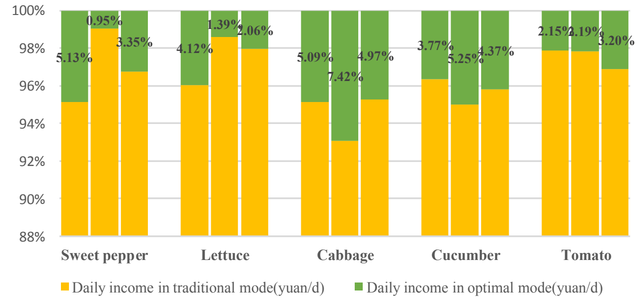

Fig.8. The greenhouse economic improvement of crop planting

IV. CONCLUSION

In this paper, a method of converting the crop growth mechanism into electricity consumption is proposed by considering the light and water requirements on crop growth in greenhouse. An agricultural load model is developed based on the crop evapotranspiration model and the daily light integral model. Power system simulation has been conducted to study the optimal operation of greenhouse with proposed agricultural load model, PV generation and battery energy storage system. Economic benefits from optimal operation of greenhouse system are quantified. The following conclusions are drawn:

The load characteristics are mainly constituted by the artificial lighting compensation system. The irrigation system of the load is relatively negligible. The irrigation system mainly reduces the waste of water resources from irrigating soil to irrigating the crop. In addition, electricity consumption of photovoltaic greenhouse can be optimized with maximum electricity cost savings of 75.93% under the proposed model. Furthermore, the overall income of agricultural production is improved by 7.43%.

The potential application of the model to guide the planning of rural distribution network construction, and the systematic approach to use the agricultural load for clean energy consumption will be investigated in the future work.

REFERENCES

[1] J. G. Liu, G. Q. Mao, A. Y. Hoekstra, H. Wang, J. H. Wang, and C. M. Zheng, "Managing the energy-water-food nexus for sustainable development," *Applied Energy*, vol. 210, no. 15, pp. 377-381, Jan. 2018.

[2] J. Y. Dai, S. Q. Wu, G. Y. Han, J. Weinberg, X. H. Xie, X. F. Wua, X. Q. Song, B. Y. Jia, W. Y. Xue, and Q. Q. Yang, "Water-energy nexus: A review of methods and tools for macro-assessment," *Applied Energy*, vol. 210, no. 15, pp. 393-408, Jan. 2018.

[3] T. Y. Wang, G. X. Wu, J. W. Chen, P. Cui, Z. X. Chen, Y. Y. Yan, Y. Zhang, M. C. Lia, D. X. Niu, B. G. Li, and H. Y. Chen, "Integration of solar technology to modern greenhouse in China: Current status, challenges and prospect," *Renewable and Sustainable Energy Reviews*, vol. 70, pp. 1178-1188, Apr. 2017.

[4] J. Y. Liu, Y. X. Chai, Y. Xiang, X. Zhang, S. Gou, and Y. B. Liu, "Clean Energy Consumption of Integrated Energy Power System Towards Intelligent Agriculture: Roadmap, Bottlenecks and Technologies," *CSEE Journal of Power and Energy Systems*, vol. 4, no. 3, pp. 273-282, Sep. 2018.

[5] Q. S. Xu, C. X. Yang and Q. G. Yan, "The peaking strategy of electric loads considering the thermal balance inertia of large-scale air conditioners," *Power System Technology*, vol. 40, pp. 156-163, Jan. 2016.

[6] F. L. Quilumba, W. Lee, J and Játiva-Ibarra, "Load Models for Flat-Panel TVs," *IEEE Transactions on Industry Applications*, vol. 50, no. 6, pp. 4171-4178, Mar. 2014.
[7] K. Mckenna, A. Keane, "Open and closed-loop residential load models for assessment of conservation voltage reduction," *IEEE Transactions on Power Systems*, vol. 32, no. 4, pp. 2995 - 3005, Jul. 2017.
[8] L. D. Wang, W. He and Z. L. Pu, "Voltage step detection and parameter identification method for general dynamic load mode," *Power System Technology*, vol. 38, pp. 2479-2483, Sep. 2014.
[9] X. Qu, X. R. Li, J. Y. Song and C. He, "An extended composite load model taking account of distribution network", *IEEE Transactions on Power Systems*, vol. 33, no. 6, pp. 7317 - 7320, Nov. 2018.
[10] J. V. Milanovic, K. Yamashita, S. M. Villanueva, S. Z. Djokic, and L. M. Korunović, "International industry practice on power system load modeling," *IEEE Transactions on Power Systems*, vol. 28, no. 3, pp. 3038 - 3046, Aug. 2013.
[11] Y. L. Zhao and Y. Gao, "The load forecasting of rural power system—based on excel regression model," *Journal of Agricultural Mechanization Research*, vol. 2, no. 36, pp. 226-228, Feb. 2014.
[12] Q. H. Lai, B. L. Mi and Z. J. Yang, "Forecasting of agricultural machine power of heilongjiang province based on artificial nerve network model," *Journal of Agricultural Mechanization Research*, vol. 4, pp. 272-274, Apr. 2005.
[13] R. F. Guo, W. J. Li, X. R. Wang, B. X. Chen, Z. K. Huang, T. Liu, X. X. Han, and Z. X. Lai, "Effect of photoperiod on the formation of cherry radish root," *Scientia Horticulturae*, vol. 244, no. 26, pp. 193-199, Jan. 2019.
[14] M. Nico, D. J. Miralles, and A. G. Kantolica, "Natural post-flowering photoperiod and photoperiod sensitivity: Roles in yield-determining processes in soybean," *Field Crops Research*, vol. 231, no. 1, pp. 141-152, Feb. 2019.
[15] Z. N. Yan, D. X. He, G. H. Niu, and H. Zhai, "Evaluation of growth and quality of hydroponic lettuce at harvest as affected by the light intensity, photoperiod and light quality at seedling stage," *Scientia Horticulturae*, vol. 248, no. 5, pp. 138-144, Apr. 2019.
[16] Y. P. Sun, Y. B. Sun, Z. C. Sun, Q. Liu, P. W. Li, and C. Z. Li, "Study on solar radiation distribution in China," *Hunan Forestry Science and Technology*, vol. 42, no. 4, pp. 43-47, Aug. 2015.
[17] X. Zhang, "Technical foundation of environmental feedback control of hydroponic lettuce based on photosynthesis simulation," *China Agricultural University*, 2017.
[18] X. P. Song, T. W. Hugh, P. Y. Tan, "Assessment of light adequacy for vertical farming in a tropical city," *Urban Forestry & Urban Greening*. vol. 29, pp. 49-57, Jan. 2018.
[19] R. C. Morrow, "LED lighting in horticulture," *Hortscience A Publication of the American Society for Horticultural Science*, vol. 43, no. 7, pp. 1947-1950, Dec. 2008.
[20] R. Hassanien, E. Hassanien, M. Li, and W. D. Lin, "Advanced applications of solar energy in agricultural greenhouses," *Renewable and Sustainable Energy Reviews*, vol. 54, pp. 989-1001, Feb. 2016.
[21] Y. Q. Xu, "Optimal Design of LED Assembled Light Source & Its Application in greenhouse plant production," *Zhejiang A&F University*, 2017.
[22] Z. S. Wang, "Optimization of winter wheat irrigation schedule in guangzhong region shanxi province by crop models," *Northwest A &F University*, 2016.
[23] X. J. Li, S. Z. Kang, J. Niu, Z. L. Huo and J. Z. Liu, "Improving the representation of stomatal responses to CO2 within the Penman–Monteith model to better estimate evapotranspiration responses to climate change," *Journal of Hydrology,* Vol. 572, pp. 692-705, May 2019.
[24] A. Ershadi, M. F. McCabe, J. P. Evans, and E. F. Wood, "Impact of model structure and parameterization on Penman-Monteith type evaporation models," *Journal of Hydrology*, vol. 525, pp. 521-535, Jun. 2015.
[25] M. M. Davis and S. Hirmer, "The potential for vertical gardens as evaporative coolers: An adaptation of the 'Penman Monteith Equation'," *Building and Environment*, vol. 92, pp. 135-141, Oct. 2015.
[26] J. D. Valiantzas, "Simplified forms for the standardized FAO-56 Penman-Monteith reference evapotranspiration using limited weather data," *Journal of Hydrology*, vol. 505, no. 15, pp. 13-23, Nov. 2013.
[27] L. Olivera-Guerra, O. Merlin, S. Er-Raki, S. Khabba, M. J. Escorihuela, "Estimating the water budget components of irrigated crops: Combining the FAO-56 dual crop coefficient with surface temperature and vegetation index data," *Agricultural Water Management*, vol. 208, no. 30, pp. 120-131, Sep. 2018.
[28] Y. Yang, Y. L. Cui, K. H. Bai, T. Y. Luo, J. F. Dai, W. G. Wang, and Y. F. Luo, "Short-term forecasting of daily reference evapotranspiration using the reduced-set Penman-Monteith model and public weather forecasts," *Agricultural Water Management*, vol. 211, pp. 70-80, Jan. 2019.
[29] V. Phogat, J. Šimůnek, M. A. Skewes, J. W. Cox, M. G. McCarthy, "Improving the estimation of evaporation by the FAO-56 dual crop coefficient approach under subsurface drip irrigation," *Agricultural Water Management*, vol. 178, pp. 189-200, Dec. 2016.
[30] S. Irmak, T. A. Howell, R. G. Allen, J. O. Payero and D. L. Martin, "Standardized ASCE Penman-Monteith: Impact of sum-of-hourly vs. 24-hour timestep computations at reference weather station sites," *Transactions of the American Society of Agricultural Engineers*, vol.48, no. 3, pp.1-15, May. 2005.
[31] J. Carroquino, R. Dufo-López, and J. L. B. Agustín, "Sizing of off-grid renewable energy systems for drip irrigation in Mediterranean crops," *Renewable Energy*, vol. 76, pp. 566-574, Apr. 2015.
[32] C. S. Li, H. Y. Wang, H. Miao, and B. Ye, "The economic and social performance of integrated photovoltaic and agricultural greenhouses systems: Case study in China," *Applied Energy*, vol. 190, pp. 204-212, Mar. 2017.
[33] China Agricultural Information Network, http://www.agri.cn/.

Zeming Li, was born in Sichuan, China. He received the B.S. degree in electrical engineering and automation from Sichuan University in 2018. He is currently pursuing the M.S. degree in power system and automation in Sichuan University, Chengdu, China. His research interests include agricultural load and distributed energy consumption.

Junyong Liu (M'17) received the Ph.D. degree from Brunel University, UK, in 1998. He is a professor in the College of Electrical Engineering and Information Technology, Sichuan University, China. His main research areas of interest are power market, power system planning, operation, stability and computer applications.

Yue Xiang (S'12-M'16) received the B.S. and Ph.D. degrees from Sichuan University, China, in 2010 and 2016, respectively. From 2013 to 2014, he was a joint Ph.D. student at the Department of Electrical Engineering and Computer Science, University of Tennessee, Knoxville, US and also a visiting scholar at the Department of Electronic and Electrical Engineering, University of Bath, UK in 2015. Now he is an associate professor in the College of Electrical Engineering and Information Technology, Sichuan University, China. His main research interests are power system planning and optimal operation, renewable energy integration and smart grids.

Xin Zhang (M'17) received the B.Eng. degree in automation from Shandong University, China, in 2006; the M.Sc. and Ph.D. degrees in electrical power engineering from The University of Manchester, U.K., in 2007 and 2010 respectively.He is a Senior Lecturer (Associate Professor) in energy systems at Cranfield University, U.K. His recent research activities include sustainable energy systems for the electrification of airports and aviation. From 2011 to 2019, he was a Power System Engineer at National Grid U.K., where he took various roles including national energy strategy, power system analysis and power market operation, mainly in the GB Electricity National Control Centre. His research interests include power system planning and operation, smart energy networks with the integration of renewable and multi-vector energy sources. He is a Chartered Engineer with the U.K. Engineering Council.

Yanxin Chai was born in Shanxi, China. She received her B.Eng. degree in electrical engineering and automation from Sichuan University, China, in 2017. She is now studying for her M.Sc. degree in electrical engineering from Sichuan University, China. Her research interests include investment and planning of distribution networks.